UDC 542.65:66.093:661.887

DOI: 10.15372/CSD2021280

Preparation of Bismuthyl (III) Fumarate Microspheres from Chloric Acid Solutions

K. V. MISHCHENKO, E. E. LUNEVA, YU. M. YUKHIN

Institute of Solid State Chemistry and Mechanochemistry, Siberian Branch of the Russian Academy of Sciences, Novosibirsk, Russia

E-mail: Mishenko.k@solid.nsc.ru

(Received June 10, 2020; revised October 13, 2020)

Abstract

The spherical microstructures of bismuthyl (III) fumarate with the composition $(BiO)_2C_4H_2O_4$ were obtained using the standard method of precipitation from solutions at 23 and 60 °C. The composition of the reaction product and its properties were studied using a complex of physicochemical methods. At 60 °C, the degree of bismuth precipitation in the product is not less than 99.8 % for the molar ratio of bismuth to fumarate ion equal to 1.5. According to IR and Raman spectroscopy data, both acidic residues of fumaric acid are deprotonated in the resulting compound, while the carboxylic groups have bidentate coordination to bismuthyl cation. The effect of temperature on the morphology of obtained compounds was studied by scanning electron microscopy and small-angle laser light scattering. According to scanning electron microscopy data, $(BiO)_2C_4H_2O_4$ obtained at 23 °C is composed of spherical particles about 10–12 μm in size, consisting of thin nanoplates about 0.1 μm thick. The data of sedimentation analysis of the powder indicate a symmetric particle size distribution with the average particle size equal to 11.7 μm. With an increase in precipitation temperature to 60 °C, particle size decreases to 3–7 μm; an asymmetric function of particle size distribution is observed, and the average size of the aggregates is 30.9 μm. A possible mechanism for the formation of $(BiO)_2C_4H_2O_4$ spherical microstructures is described as a process combining Ostwald ripening and self-assembling. According to the data of thermal and XRD analyses, the product of thermal decomposition of bismuthyl fumarate at a temperature of 450 °C is a monoclinic modification of Bi_2O_3.

Keywords: bismuthyl (III) fumarate, microspheres, oxide, hydrochloric solutions, precipitation

INTRODUCTION

Bismuth-containing pharmaceutical preparations are widely used to treat infections caused by some bacterial, especially *Helicobacter pylori* – etiologic agents of such diseases as gastritis, stomach ulcer or cancer. Anti-ulcer activity of bismuth-containing preparations is mainly explained by bismuth precipitation on ulcer surface as a result of the formation of strong bismuth-containing glycoprotein complexes [1].

Derivatives of fumaric acid have been known long age and are used to treat psoriasis and autoimmune diseases [2]. The salts of fumaric acid (for example, magnesium, calcium, iron or sodium fumarates) are used as an antihypoxic agents in infusion media to maintain and correct energy exchange in cells, and for substitutive therapy to recover the level of lacking microelements in the organism [3]. In this connection, the salt of bismuth with fumaric acid along with other bismuth-containing salts of carboxylic acids may be considered as a potential medicinal substance.

A standard approach to the synthesis of bismuth salts is their precipitation from the solutions of mineral acids. Nitric solutions of bismuth

are usually used in these processes. A disadvantage of this procedure is co-precipitation of solid bismuth oxohydroxonitrates of different compositions with an increase in pH and temperature. In our opinion, it is reasonable to carry out precipitation from bismuth-containing chloric acid solutions because their dilution with water does not lead to the formation of double salts containing perchlorate ions. These solutions are usually used as model systems to investigate the composition of deposition products. It is known that bismuth in the concentration above 0.1 mol/L is present in the solutions of chloric acid (pH < 1) in the form of polycation $[Bi_6O_4(OH)_4]^{6+}$ [4, 5].

A literature survey on the synthesis and properties of the salts of bismuth with fumaric acid did not give any results. For this reason, the authors of the present work assumed that this is a new compound, it has not been synthesized previously in the solid form, and thus its composition and structure are not studied yet.

The goal of the present work was to apply the standard methods of investigation to study the composition, morphology, and thermal properties of the products of bismuth precipitation obtained through the interaction of the chloric solutions of bismuth with the solutions of fumaric acid depending on the ratio of bismuth to fumaric ion and process temperature (23 and 60 °C).

EXPERIMENTAL

The initial bismuth-containing solution was prepared by dissolving Bi_2O_3 (especially pure reagent grade 13-3) in chloric acid (chemically pure reagent grade, concentration 6 mol/L). Bismuth concentration in solution $C(Bi^{3+})$ was 5 mol/L. The concentration of free chloric acid was 0.95 mol/L, which was determined by means of acid-base titration after preliminary bismuth masking by complexone III [6].

The necessary amount of bismuth-containing solution was added dropwise into the solution of fumaric acid (0.04 mol/L) 250 mL in volume and mixed for 1 h. Investigation of the deposition of bismuthyl (III) fumarate was carried out at a temperature of 23 and 60 °C, usually used for the synthesis of bismuth compounds. Preliminary studies provide evidence that 4 h is sufficient to achieve equilibrium in the system at a temperature of 60 °C, while 8 h is necessary at a temperature of 23 °C. The mother solution was separated by decanting, and the white precipitate was washed twice with distilled water at 60±2 °C and dried in the air at room temperature.

X-ray phase analysis (XPA) of precipitation products was carried out by means of powder X-ray diffraction using a D8 Advance diffractometer (Bruker, Germany) with CuK_α radiation (λ = 1.5418 Å). Phase identification was performed using the powder database PDF-4+ (2011). Sample morphology was studied using scanning electron microscopes (SEM) TM1000 and 3400 N (Hitachi, Japan). Differential thermal analysis (DTA) was carried out with the help of a synchronous thermoanalytical complex STA 449 F1 Jupiter (Netzsch, Germany) in the dynamic mode under heating in the atmosphere of Ar/O_2 (with the percentage of 80 : 20). The IR and Raman spectra were recorded with an Infralyum FT-801 Fourier spectrometer (LC NPF Lyumeks-Sibir, Russia) within the medium frequency range 400–4000 cm^{-1}. Samples were prepared as tablets with annealed KBr. The content of C and H in the samples was determined with the help of a CNH-analyzer with modified tube in the Sharing Equipment Centre at the Novosibirsk Institute of Organic Chemistry SB RAS (Novosibirsk) [7]. The specific surface area of the obtained samples was studied by means of low-temperature nitrogen adsorption at 77 K (Sorbtometr-M analyzer, CC Katakon, Russia). Particle size was determined with the help of a laser particle analyzer Micro-Sizer 201 BA Instruments (Russia). Before analysis, the samples were subjected to ultrasonic treatment (200 W) for 30 s. Macro amounts of Bi (III) in solid products were determined through titration with the solution of complexone III in the presence of xylenol orange as an indicator, and micro amounts were determined by means of photocolorimetry with sodium iodide [8].

RESULTS AND DISCUSSION

Bismuth precipitation was carried out at a temperature of 23 or 60 °C with different molar ratios of the amounts of bismuth and fumaric acid introduced into the reaction: $n(Bi^{3+}/C_4H_2O_4^{2-})$. Results of the effect of n value on the degree of bismuth recovery (R_{pr}) into precipitate and the compositions of reaction products are presented in Table 1. Bismuth is quantitatively precipitated from solution under the following conditions: temperature 23 °C, n = 0.25, 0.50. At increased precipitation temperature (60 °C) the high degree of bismuth recovery into precipitate was detected within the

TABLE 1

Conditions for obtaining bismuthyl (III) fumarate, precipitation degree and the composition of reaction products ($C(Bi^{3+})$ = 5 mol/L)

$V(Bi^{3+})$, mL	V_{sol}, mL	$n(Bi^{3+}/C_4H_2O_4^{2-})$	T, °C	$[H^+]$, mol/L	R_{pr}, %	Composition of products
0.5	249.5	0.25	23	0.037	99.87	$C_4H_4O_4$ $(BiO)_2C_4H_2O_4$
1	249.0	0.5	23	0.052	99.82	$C_4H_2O_4$ $(BiO)_2C_4H_2O_4$
2	248.0	1.0	23	0.062	87.56	$C_4H_2O_4$ $(BiO)_2C_4H_2O_4$
4	246.0	2.0	23	0.099	87.08	$C_4H_2O_4$ $(BiO)_2C_4H_2O_4$
6	244.0	3.0	23	0.158	59.81	$C_4H_2O_4$ $(BiO)_2C_4H_2O_4$
0.4	249.6	0.2	60	0.045	99.60	$(BiO)_2C_4H_2O_4$
0.8	249.2	0.4	60	0.061	99.56	$(BiO)_2C_4H_2O_4$
1.6	248.4	0.8	60	0.076	99.16	$(BiO)_2C_4H_2O_4$
3	247.0	1.5	60	0.123	99.02	$(BiO)_2C_4H_2O_4$
4	246.0	2.0	60	0.140	98.80	$(BiO)_2C_4H_2O_4$
6	244.0	3.0	60	0.191	62.66	$(BiO)_2C_4H_2O_4$

Note. V is volume; $\boldsymbol{n}$ is molar ratio; T is temperature; R_{pr} is the degree of recovery into precipitate; C, $[H^+]$ are concentrations.

studied range n = 0.2–2.0. With an increase in n, a decrease in R_{pr} is observed. This is likely to be due to an increase in the concentration of hydrogen ions in the solution, which prevents salt precipitation. The low recovery degree observed for n = 3 is evidence of the lack of fumaric acid.

Bismuth in chloric solutions with bismuth concentration more than 0.1 mol/L is in the form of polycation $[Bi_6O_4(OH)_4]^{6+}$ [4, 5]. This complex is destroyed during dilution with water, and at pH 0.3 bismuth is present in the form of cations Bi^{3+}, $Bi(OH)^{2+}$, $(BiO)^+$ [9]. Because of this, it may be assumed that the formation of bismuthyl (III) fumarate occurs in the presence of fumaric acid according to the reaction:

$$2(BiO)^+ + C_4H_4O_4 \rightarrow (BiO)_2C_4H_2O_4 + 2H^+ \quad (1)$$

The composition of the resulting compound was studied with the help of chemical and X-ray phase analysis (Fig. 1). For n = 0.25–2.0 and precipitation temperature 23 °C, the synthesized white powders are multiphase samples. The X-ray diffraction patterns of intermediate (not washed with water) samples contain the reflections of fumaric acid [10] with the basic diffraction peaks corresponding to interplanar spacing (d): 3.9, 3.6, 3.45, 3.10, 3.04, 2.37, 2.32, 2.14 Å (see Fig. 1, curve *1*), and a number of reflections with d 10.47, 3.36, 2.98, 2.82 Å (see Fig. 1, curve *2*), non-identified in the ICDD database. The presence of the crystal phase of fumaric acid in the sample before washing is connected with its capture from the mother solution during the separation of precipitate at the filtration stage and subsequent crystallization at the stage of drying. For the samples washed with distilled water, independently of the conditions of their synthesis, only reflections with interplanar spacing d 10.47, 3.36, 3.57, 3.47, 3.36, 2.98, 2.82, 2.73, 2.66, 2.61, 2.47, 2.31, 2.19, 2.08, 1.99, 1.93, 1.92, 1.76 Å remain in the diffraction patterns (see Fig. 1, curve *3*). This fact allows us to state that the obtained solid product is bismuthyl (III) fumarate.

According to chemical analysis, the concentration of Bi^{3+} ions in the product obtained at n = 2 (60 °C) is 73.7 mass %. This value is very close to the theoretical one (74.1 mass %) for bismuthyl fumarate with the composition $(BiO)_2C_4H_2O_4$. The content of other elements in the sample is, mass %: C – 8.58 (calculated value: 8.51), H – 0.37 (calculated value: 0.35).

Thermal analysis of the obtained compound in the mode of linear heating to a temperature of 450 °C in the atmosphere of Ar/O_2 provides evidence of its decomposition to bismuth oxide according to the equation:

$$(BiO)_2C_4H_2O_4 + 3O_2 \rightarrow Bi_2O_3 + 4CO_2\uparrow + H_2O \quad (2)$$

According to XPA data (see Fig. 1, curve *4*), the final product of oxidative thermolysis in the air is monoclinic bismuth oxide. The phase transformations of bismuthyl (III) fumarate during

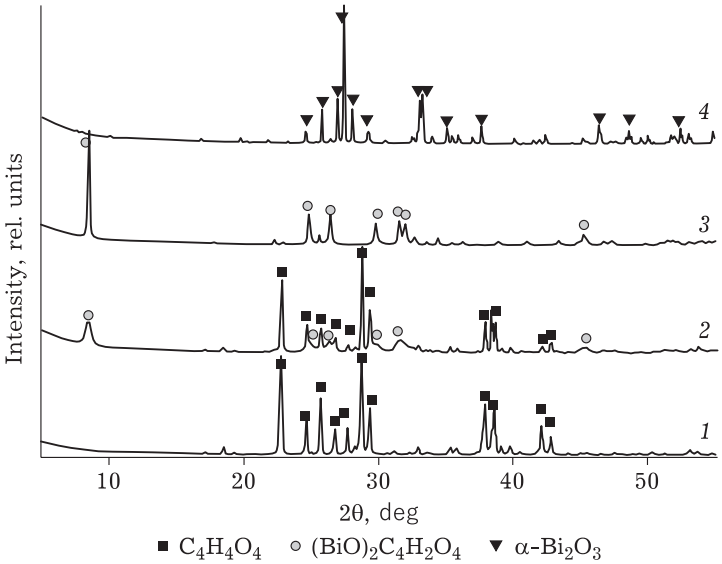

Fig. 1. X-ray diffraction patterns of initial fumaric acid (*1*) and the products of precipitation from chloric solutions at $n = 2$, $T = 23$ °C before (*2*) and after washing with water at 60 °C (*3*); α-Bi_2O_3 (PDF #71-2274) obtained after thermolysis at 450 °C in the air (*4*).

thermal decomposition were described in more detail in [11]. The experimentally determined mass change Δm (17.5 mass %) corresponds to the theoretical value Δm_t (17.4 mass %), calculated for the sample with the composition $(BiO)_2C_4H_2O_4$.

SEM images of bismuthyl (III) fumarate freshly precipitated from the chloric solution provide evidence that the sample obtained at 23 °C and washed with water is represented by microstructures in the form of spherical particles 10–15 μm in size, composed of smaller nanoplates (Fig. 2, *a*). The specific surface area of the product is 8.7 m^2/g. The sample obtained at 60 °C contains particle agglomerates 2–4 μm in size, composed of plates less than 0.1 μm thick (see Fig. 2, *b*). In this case, the specific surface area is 9.9 m^2/g. It may be assumed on the basis of SEM data (see Fig. 2, *b*, *c*) that spherical microstructures are formed with the help of spatial self-arrangement described in [12] for bismuthyl oxocarbonate $(BiO)_2CO_3$. At the initial stage, nanoparticles of bismuthyl (III) fumarate are formed in the interac6tion of Bi^{3+} with $C_4H_2O_4^{2-}$ anions, then nanoplates are formed during Ostwald ripening. It is known that according to Gibbs–Thomson law larger particles are characterized by lower solubility than smaller ones because of the difference in Gibbs energies, which results in the growth of larger particles due to the dissolution of fractured ones. It is also considered that the decisive part in the morphology of the reaction product is played by its crystal structure. Increased intensity of the reflection with interplanar spacing 10.47 Å in the diffraction pattern of bismuthyl (III) fumarate is characteristic of bismuth compounds with layered structure and the developed (001) plane [13, 14]. Among bismuth compounds, there are the compounds with Sillen structure [15] in which (001) planes containing $[Bi_2O_2]^{2+}$ layers alternate with anion layers. As described in [14], (110) planes of bismuth sublattice contain a larger number of dangling bonds, therefore, according to Gibbs-Thomson law, they are characterized by higher chemical potential. The internal anisotropic growth leads to the preferential formation of nanoplates along the (001) plane as a consequence of faster growth of (110) planes. At the final stage of the formation of bismuthyl (III) fumarate microstructures, self-assembling of the nanoplates into spherical particles occurs.

Small-angle scattering of laser radiation was used to study the particle size of the powders. It was established that 62.6 % of the particles synthesized at 60 °C form aggregates 19–43 μm in size, which agrees with the data of the microscopic examination of the samples. The values of standard deviation provide evidence of a broad range of particle and aggregate size distributions [16], that is, both systems are generally polydisperse (Table 2). The histogram of the samples obtained at 23 °C is symmetrical, but the

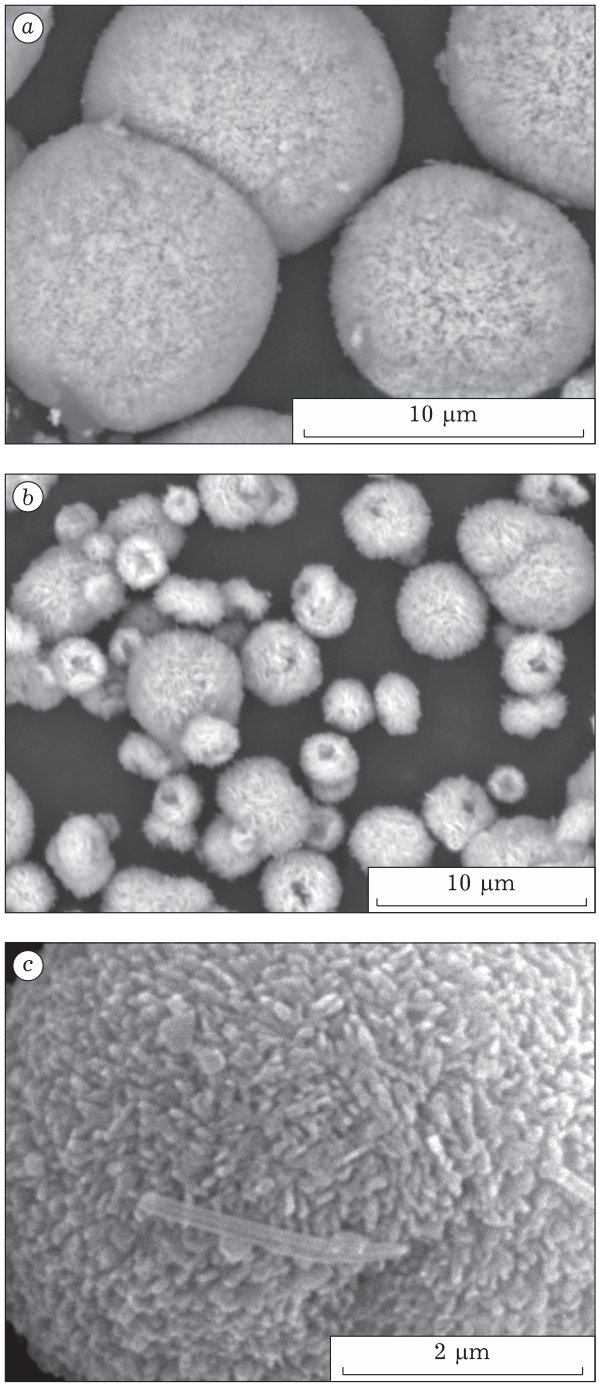

Fig. 2. SEM images of the samples of bismuthyl (III) fumarate obtained at 23 (*a*, *c*) and 60 °C (*b*), washed with water.

value of asymmetry factor points to insufficient segregation of the sample, that is, no fraction corresponding to a narrow size range may be distinguished. The value of asymmetry factor for the powder obtained at 60 °C is characteristic of low-symmetrical distribution, which is the evidence of the presence of aggregates not identical in their size to each other.

The IR and Raman spectra of the obtained salt were compared with the spectra of initial fumaric acid [10]. A number of characteristic bands [17, 18] that are observed in the IR spectrum of fumaric acid (Table 3) are absent from the spectrum of the salt under investigation. The stretching vibrations of O–H bonds in carboxylic groups of fumaric acid appear as a weak band with the maximum at 3084 cm^{-1}. In the region of 3000–2500 cm^{-1}, there is a group of bands overlapping with the bands of the stretching vibrations of C–H bonds (a weak band at 3078 cm^{-1} in the Raman spectrum) and those corresponding to the vibrations of O–H•••H groups bound in dimers by hydrogen bonds [19]. The stretching vibrations of C=C bonds manifest themselves as a high-intensity band at 1668 cm^{-1} (in the Raman spectrum), while the vibrations of C=O bonds in carboxylic groups are responsible for a broad intense band with the maximum at 1677 cm^{-1} (in the IR spectrum). A slight shift of the C=O band to lower frequencies is an evidence of the presence of dimer carboxyl groups, while an increased intensity is the evidence of trans-orientation of the molecules and conjugation of C=O and C=C bonds [17]. Medium-intensity bands in the region of 1420–1400 cm^{-1} (1410 cm^{-1} in the Raman spectrum) may be attributed to the symmetrical vibrations of carboxylic groups $(COO)^-$ bound in dimers [18]. The presence of combined frequencies (usually a doublet) in the region of 1320–1210 cm^{-1} (in IR and Raman spectra) is due to in-plane bending vibrations of C–H bonds and O–H bonds of hydroxyl in the carbonyl group, which are tightly conjugated with the stretching vibrations of C–O [20]. Next to the band of

TABLE 2

Results of dispersion analysis of the samples of bismuthyl (III) fumarate

T, °C	Average size of 50 mass % particles and aggregates (D_{50}), μm	Average size of particles and aggregates (*D*), μm	Standard deviation*	Asymmetry factor*
23	11.6	11.7	2.137 (2–4)	−0.039 (−0.43 ... 0.43)
60	26.2	30.85	24.1 (>16)	3.489 (>1.3)

* The range of values reported in [16] is indicated in parentheses.

stretching vibrations of C–CO^- bond, with the maximum at 1011 cm^{-1}, there is a broad medium-intensity band within absorption region 980–800 cm^{-1} (980–890 cm^{-1} in the Raman spectrum), characteristic of out-of-plane bending vibrations of O–H, C–O and C–H [17, 20]. Two medium-intensity bands at 634 and 549 cm^{-1} correspond to wagging and rocking bending vibrations of carboxylic group, respectively [18, 20].

For the salt of fumaric acid, a comparison of the characteristic bands in IR and Raman spectra was carried out also with the spectra of bismuth formiate, fumarates of potassium, silver and rare earth elements (III) [20–23]. Considering the IR spectrum of the synthesized salt. one may notice the absence of absorption bands characteristic of the carbonyl group of fumaric acid, and the appearance of two bands with the maxima at 1511 and 1396 cm^{-1} (1508 and 1402 cm^{-1} in the Raman spectrum), which correspond to the asymmetric and symmetric vibrations of carboxylate anion (COO^-). The difference between the wavenumbers $\Delta(n_{as} - n_s)$ for COO^- is equal to 116 cm^{-1} (for sodium fumarate – 169 cm^{-1}), which allows us to conclude that bonds of carboxylic groups of fumaric acid are in bidentate coordination to bismuthyl (III) cations with incomplete leveling of bond lengths in the carboxylate anion, similarly to the fumarates of rare earth metals [22]. The shift of the band of the stretching vibrations of double bond by 34 cm^{-1} in the Raman spectrum of the salt also may point to the substitution of the proton of carboxylic group. If we assume that one non-dissociated carboxylic group –COOH is present in the compound under consideration, then we would observe a band in the region of 1715–1690 cm^{-1}. This band was not detected in the spectrum of the synthesized compound, so we may assume that carboxylic groups of fumaric acid are twice deprotonated. Two absorption bands at 1202 cm^{-1} (1270 cm^{-1} in the Raman spectrum) and 974 cm^{-1} relate to in-plane and out-of-plane bending vibrations of C–H groups. A weak absorption band at 984 cm^{-1} in the Raman spectrum corresponds to the stretching vibrations of C–C bonds [20]. The scissor bending vibrations of carboxylate anion are responsible for a strong and weak band with the maxima at 801 cm^{-1} (IR spectrum) and 758 cm^{-1} (Raman spectrum), respectively, while

TABLE 3

Assignment of the bands in IR and Raman spectra of fumaric acid and bismuthyl (III) fumarate

Characteristic absorption bands in the spectra, cm^{-1}				Band assignment
IR	Raman	IR	Raman	
Fumaric acid		Bismuthyl (III) fumarate		
3084	–	–	–	ν(O–H)
3000–2500	–	–	–	dimers bound through H-bonds [19]
–	3071	–	3068	ν(C–H)
–	1698	–	1652	ν(C=C) [21]
1674	1607	–	1603	ν(C=O) [20], including dimers
–	–	1511	1550 1508	$\nu_{as}(COO^-)$
1420 1403sh	1410	1396	1402	$\nu_s(COO^-)$, ν(C=O) [20]
1320–1200	1279	1202	1270	ν(C–O), $\delta(OH)_{ip}$, $\delta(C–H)_{ip}$
1011 921sh 904	979sh 956 912	974 891sh 831sh	984 905	$\nu(C–CO_2)$ [20, 21], $\delta(C–H)_{oop}$, $\delta(O–H)_{oop}$, $\delta_\gamma(C–O)$ [19]
780sh 720sh	–	801	758	$\delta_s(COO^-)$ [20]
643 581	695	658 580	644	$\omega(COO^-)$ [21]
549sh	451	–	437	$r(COO^-)$ [21]
–	–	519	–	ν(Bi–O) [23]

Notes. 1. Vibrations: ν – stretching (index s relates to the symmetric, as – to asymmetric vibration), δ – bending (index s relates to scissor vibrations, γ – torsional), ω – wagging, ρ – twisting, ip – in-plane, oop – out-of-plane. 2. Sh is shoulder. 3. Dash means the absence of absorption.

wagging vibrations correspond to the bands at 658 and 581 cm^{-1} (IR spectrum) and 644 cm^{-1} (Raman spectrum) [21]. A broad medium-intensity band with the maximum at 519 cm^{-1} in the IR spectrum may be related to the stretching vibrations of Bi–O bond [23].

CONCLUSION

In the present work, bismuthyl (III) fumarate was obtained by precipitation from chloric solutions, and the procedure for the synthesis of the salt at different temperatures is described. The composition of the product is confirmed on the basis of the data of chemical analysis, DTA, XPA, IR and Raman spectroscopy. Results of the investigation provide evidence that the addition of the chloric solution of bismuth into the solution of fumaric acid, independently of its concentration, leads to the formation of twice deprotonated salt of fumaric acid having the composition $(BiO)_2C_4H_2O_4$. It is also established that the degree of bismuth precipitation increases with an increase in the concentration of fumaric acid and process temperature. It is reasonable to carry out the synthesis of bismuthyl (III) fumarate from chloric solutions with the stoichiometric molar ratio bismuth/fumarate ion (n = 2) and process temperature 60 °C to decrease the consumption of fumaric acid.

It is established with the help of scanning electron microscopy that microstructures of bismuthyl (III) fumarate obtained at 23 and 60 °C have spherical shapes and are composed of crystal nanoplates. According to the data of low-temperature nitrogen adsorption, the specific surface area of the samples is 8.7 and 9.9 m^2/g, respectively. Monoclinic modification of bismuth oxide is formed in the oxidative thermolysis of bismuthyl (III) fumarate at a temperature of 450 °C.

Acknowledgements

The work was carried out within the State Assignment for the ISSCM SB RAS (Project No. AAAA-A17-117030310277-6).

REFERENCES

1 Li H., Sun H., Recent advances in bioinorganic chemistry of bismuth, *Current Opinion in Chemical Biology*, 2012, Vol. 16, P. 74–83.
2 Popova E. V., Boyko A. N., Orlova E. V., Dimethylfumarate in therapy of remittent disseminated sclerosis [in Russian], *Zhurn. Nevrologii i Psikhiatrii*, 2016, Vol. 116, No. 10-2, P. 68–72.
3 Kharitonova M. V., Zheltova A. A. Iezhitsa I. N., Ozerov A. A., Spasov A. A., Studies of the efficiency of some organic salts of magnesium in treating experimental hypomagnesia [in Russian], *Vestn. OGU*, 2011, Vol. 134, No. 15, P. 153–155.
4 Baes C. F., Mesmer R. E., The hydrolysis of cations, NY: Wiley, 1976. 512 p.
5 Sandwall B., An X-ray diffraction study of the hexanuclear complex of Bi (III) in aqueous perchlorate solution. Determination of the oxygen positions, *Acta Chem. Scand.*, 1980, Vol. 34A, P. 93–98.
6 Polyak E. A., Musikhin R. N., Rodionova L. A., Determination of free acid in the solutions of salts of complicated composition prone to hydrolysis [in Russain], *Zhurn. Analit. Khimii*, 1970, Vol. 25, No. 12, P. 2447–2450.
7 Fadeeva V. P., Tikhova V. D., Nikulicheva O. N., Elemental analysis of organic compounds using automatic CHNS-analyzers [in Russian], *Zhurn. Analit. Khimii*, 2008, Vol. 63, No. 11, P. 1197–1210.
8 Korostylev P. P., Photometric and Complexonometric Analysis in Metallurgy (a Handbook) [in Russian], A. I. Busev (Ed.), Moscow, Metallurgiya, 1984. 272 p.
9 Milanov M., Resh F., Khalkin V. A., Khenniger Yu., Kim Kh. Ch., Hydrolysis of Bi (III) in aqueous solutions [in Russian], *Radiokhimiya*, 1987, Vol. 29, No. 1, P. 21–28.
10 Suzuki Y., Muraishi K., Matsuki K., Thermal behavior of dicarboxylic acids. Determination of melting points by DTA, *Thermochimica Acta*, 1992, Vol. 211, P. 171–180.
11 Mishchenko K. V., Gerasimov K. B., Yukhin Y. M., Thermal decomposition of some bismuth oxocarboxylates with formation of β-Bi_2O_3, *Materials Today: Proceedings*, 2020, Vol. 25, No. P3, P. 391–394.
12 Cheng H., Huang B., Yang K., Wang Z., Qin X., Zhang X., Dai Y., Facile template-free synthesis of hierarchical microflowers and their associated photocatalytic activity, *ChemPhysChem*, 2010, Vol. 11, P. 2167–2173.
13 Duan F., Zheng Y., Liu L., Chen M., Xie Y., Synthesis and photocatalytic behavior of 3D flowerlike bismuth oxide formate architectures, *Mater. Lett.*, 2010, Vol. 64, P. 1566–1569.
14 Aurivillius B., X-ray studies on bismuth oxide acetate $CH_3COO{\bullet}OBi$ and related compounds, *Acta. Chem. Scand.*, 1955, Vol. 9, No. 7, P. 1213–1218.
15 Sillen L. G., Uber eine familie von oxyhalogeniden, *Naturwiss.*, 1942, Vol. 470, No. 22, P. 318–324.
16 Blott S. J., Pye K., GRADISTAT: A grain size distribution and statistics package for the analysis of unconsolidated sediments, *Earth Surf. Process. Landf.*, 2001, Vol. 26, P. 1237–1248.
17 G. Socrates., Infrared and Raman Characteristic Group Frequencies: Tables and Charts, 3rd Ed. Wiley, 2004. 366 p.
18 Bellamy L., The Infra-Red Spectra of Complex Molecules, 1st Ed., Springer, Netherlands, 1975. 433 p.
19 Timakova E. V., Afonina L. I., Yukhin Yu. I., Bulina N. V., Volodin V. A., Preparation of bismuth (III) malates by precipitation from nitrate solutions, *Chemsitry for Sustainable Development*, 2017, Vol. 25, No. 3, P. 293–300.
20 Schulte J. P., Grass S., Treuel L., Adsorption of dicarboxylic acids onto nano-structured silver surfaces – surface-enhanced Raman scattering studies of pH-dependent adsorption geometries, *J. Raman Spectros.*, 2013, Vol. 44, P. 247–254.
21 Maury L., Bardet L., Brunel R., Vierne R., Spectres Raman du monocristal de fumarate de potassium dihydraté, $K_2H_2C_4O_4$, $\cdot$ $2H_2O$, *J. Raman Spectros.*, 1981, Vol. 11, No. 1, P. 14–19.
22 Ionashiro E. Y., Caires F. J., Siqueira A. B., Lima L. S., Carvalho C. T., Thermal behaviour of fumaric acid, sodium fumarate and its compounds with light trivalent lanthanides in air atmosphere, *J. Therm. Anal. Calorim.*, 2012, Vol. 108, P. 1183–1188.
23 Gattow G., Sarter K., Bismuth(III)-formate, *Z. Anorg. Allg. Chem.*, 1980, Vol. 463, P. 163–166.